ELSEVIER

Catalysis Today 43 (1998) 101–110

CATALYSIS TODAY

Supported VPO catalysts for selective oxidation of butane III: Effect of preparation procedure and SiO_2 support

J.M.C. Bueno[a], G.K. Bethke[b], M.C. Kung[b], H.H. Kung[b,*]

[a] *On leave from DEQ/UFSCar, Caixa Postal 676, 13560, Sao Carlos, (SP), Brazil*
[b] *Department of Chemical Engineering, Ipatieff Laboratory, Northwestern University, Evanston, IL 60208, USA*

Abstract

The effects of the nature of silica support and removal of soluble vanadium species by ethanol on the catalytic properties of silica-supported VPO catalysts were investigated. Ethanol preferentially removes V^{+5} species. For a silica-supported sample of *P/V* ratio much lower than two, ethanol treatment resulted in a sample of higher *P/V* ratio and higher selectivity for maleic anhydride in butane oxidation. The crystalline VPO phases formed differed on a hydrophobic vs. hydrophilic silica. $(VO)_2P_2O_7$ could be formed more easily on the former support. Interestingly, for all silica-supported catalysts, the maleic anhydride selectivity depended much more strongly on the *P/V* ratio than on the method of preparation, the nature of the silica, or the crystalline VPO phase present.

Keywords: VPO catalysts supported; Butane oxidation on supported VPO catalyst; Maleic anhydride by butane oxidation; Preparation of supported VPO catalysts

1. Introduction

Currently, the selective oxidation of butane to maleic anhydride (MA) is the only large volume, commercially-practiced chemical synthesis by oxidation of an alkane [1]. The catalyst used for this reaction consists primarily of unsupported vanadyl pyrophosphate, $(VO)_2P_2O_7$. Supported catalysts, however, offer many potential advantages over their unsupported counterparts: (1) increased surface area to volume ratio of the active phase, (2) increased mechanical strength and (3) improved heat transfer characteristics. Although many researchers have attempted to prepare supported vanadium phosphorus oxide (VPO) catalysts, the resulting materials exhibited much lower MA selectivity compared to unsupported catalysts [2–5]. In our earlier studies [6–9], we found that on the SiO_2-supported catalysts, the MA selectivity depends on the nominal *P/V* ratio of the catalyst. Catalysts with $P/V \sim 1$ have about 25% selectivity to MA, much lower than the typical value of about 70% achieved over unsupported $(VO)_2P_2O_7$, but increases to 50–55% for catalysts with $P/V \sim 2$ [1,6]. Furthermore, interaction between VPO and the silica support hinders the formation of $(VO)_2P_2O_7$ and promotes the formation of $VOPO_4$-like phases. The latter observation suggests that, perhaps, the strong VPO–SiO_2 interaction has resulted in the presence of a much higher than optimal V^{+5}/V^{+4} concentration in the supported catalysts leading to poor MA selectivity [6]. If so, it might be possible to prepare supported

*Corresponding author.

0920-5861/98/$32.00
PII S0920-5861(98)00138-2

$(VO)_2P_2O_7$ and/or obtain catalysts of higher MA selectivities by: (1) using different preparation procedures, such as extracting V^{+5} compounds from the supported catalysts with ethanol; or (2) preparing samples with hydrophobic silica, the surface of which is covered by siloxane groups to minimize VPO–SiO_2 interaction. Here, we report the results of these experiments.

2. Experimental

2.1. Catalyst preparation

2.1.1. Silica

Three types of silica were used. For investigations of ethanol extraction, Davison silica, grade 62 (300 m^2/g), mesh 120–150, was used. Before use, the silica was washed with 1 N nitric acid to remove cationic impurities [10]. Catalysts prepared on this silica are labeled VPO/SiO_2-D. The silica used to investigate the VPO–SiO_2 interaction was Cab-O-Sil fumed silica. These fumed silicas consisted of nearly spherical silica particles that form three-dimensional, branched chain aggregates that can further intertwine to form agglomerates of the chains. The hydrophilic silica used was Cab-O-Sil L-90 (90 m^2/g) [11]. Catalysts prepared with this silica are labeled VPO/SiO_2–OH. The hydrophobic silica used was Cab-O-Sil TS-720 (100 m^2/g) [11]. Terminal silanol groups of this silica have been replaced by chains of dimethyl siloxane ($-O[Si(CH_3)_2O]_nSi(CH_3)_3$). Catalysts prepared with this silica are labeled VPO/SiO_2–CH_3. Both types of silica were used as received.

2.1.2. *VPO/SiO_2-D catalysts*

The VPO precursor was prepared by reduction of V_2O_5 in water by HCl at 100°C ($\sim$ 72 h) following the method described by Centi et al. [12]. H_3PO_4 (85%) was then added to the solution, and the mixture was refluxed for 1 h to obtain solution A. The *P/V* ratio was varied by adjusting the amount of H_3PO_4 added during the synthesis of solution A. Solution A was then directly used for impregnation at loadings of 8.4 wt% vanadium. A bulk sample was prepared by evaporation of solution A. The supported samples obtained are labeled *VPO/SiO_2-D-y*, and the bulk sample is labeled *Bulk-y*, where *y* represents the nominal *P/V* ratio before activation. Some samples were washed with ethanol before activation. They are labeled *VPO/SiO_2-D-yW*, where *y* represents the *P/V* ratio before ethanol washing. The samples were activated under reaction conditions by first heating to 100°C at 2°C/min in a total flow of 41 ml/min. The samples were then heated to 380°C and held at that temperature for 8 h. The temperature was then increased to either 475°C or 550°C and held at that temperature for an additional 8 h. The temperature was then lowered to the reaction temperature.

2.1.3. *VPO/SiO_2–OH and VPO/SiO_2–CH_3 catalysts*

For samples VPO/SiO_2–OH, solution A with a *P/V* ratio of 1.1 was used directly for impregnation. For samples VPO/SiO_2–CH_3, the same solution was first evaporated in air to decrease the water content, then redispersed with acetone. The acetone solution was then used for impregnation. Loadings were 15 g V/100 g SiO_2. Bulk samples were obtained by evaporation of solution A to a brown solid and are labeled *Bulk*.

The impregnated samples and the bulk precursor were activated by first calcining in air at 500°C for 24 h. Such derived catalysts are labeled *–A*. Some of the samples were further heated in flowing N_2 (200 ml/min) at 770°C for 2 or 24 h. The resulting catalysts are labeled *–Nx*, where *x* indicates the time (in h) for which the sample remained in the nitrogen treatment.

2.2. Catalyst characterization

X-ray diffraction (XRD) patterns were collected in air with a Rigaku diffractometer using $Cu_{K\alpha}$ radiation with a Ni filter. For the VPO/SiO_2-D catalysts, the patterns were collected in an air-tight sample cell. After the various pretreatments, the samples were quickly loaded into the cell under ambient conditions. For the other catalysts, the patterns were collected under ambient conditions. Laser Raman (LRS) spectra were collected using the 514.5 nm line of the Coherent INOVA 70-2 Ar ion laser and spectrometer previously described [13]. Spectra were collected either in situ (0.99/10.2/88.81 = C_4H_{10}/O_2/He, 400°C) or under ambient conditions at a laser power of either 20 or 25 mW. Samples that had been used previously for reaction in a microreactor were used to collect spectra

under in situ conditions to avoid possible complications due to transient behavior. To verify that no changes occurred during the in situ LRS collection, three spectra for each sample were collected: first at room temperature, then at 400°C, and finally after cooling to room temperature. Phosphorus and vanadium concentrations were determined by inductively coupled plasma atomic emission spectroscopy. Diffuse reflectance spectra (DRS) were obtained in air with a Cary 5 Spectrometer using polytetrafluoroethylene as a reference.

2.3. Reaction

Steady-state reactions were conducted in a tubular, fused silica microreactor near atmospheric pressure. Reactions were typically carried out with a C_4H_{10}/O_2/He feed of 2/20/78 or 2/24/74 at a total flow rate of 40–70 ml/min with 0.15–0.8 g of catalyst. When necessary, the amount of catalyst and the total flow rate were adjusted to maintain similar W/F values. Carbon balances were typically between 100% and 104%. The catalyst bed was supported on acid-washed quartz wool, and the remaining volume of the reactor was filled with fused silica chips to minimize gas-phase reactions. On-line gas chromatography employing a combination of Carbosphere, VZ-7, and Carbowax on Graphpac GB columns in parallel was used to analyze the reaction products as previously described [6].

3. Results

3.1. Effect of ethanol extraction and P/V ratio

Three VPO/SiO_2-D catalysts of different *P*/*V* ratios were prepared and studied. The compositions of these catalysts before and after ethanol extraction, analyzed post-reaction, are listed in Table 1. As the *P*/*V* ratio of the catalysts increased, the fraction of vanadium extracted with ethanol decreased. Analysis of ethanol after extraction showed dissolution of a small amount of phosphorus also. For sample VPO/SiO_2-D-2.4, only a small amount of vanadium was extracted.

3.1.1. Catalyst characterization

The XRD pattern of the bulk precursor corresponded to $VOHPO_4 \cdot 0.5H_2O$ [14]. After activation at 380°C, $(VO)_2P_2O_7$ was formed with trace amounts of α_{II}-$VOPO_4$, δ-$VOPO_4$ and γ-$VOPO_4$. Hutchings et al. [15] have shown similar transformations using laser Raman spectroscopy. After activation at 475°C, the sample showed patterns of only $(VO)_2P_2O_7$ and α_{II}-$VOPO_4$.

Table 1
Composition of VPO/SiO_2-D catalysts (post-reaction)

Sample	*P*/*V*	Wt% *V*/SiO_2	*P*/*V* in ethanol	$V_{extracted}/V_{initial}$
D-1.1	1.08	8.2	—	—
D-2.0	1.96	8.1	—	—
D-2.4	2.38	8.3	—	—
D-1.1W	1.72	4.6	0.39	0.481
D-2.0W	2.00	7.7	1.51	0.068
D-2.4W	2.30	8.0	6.02	0.021
Bulk-1.1	1.08	—	—	—

Before activation, the VPO/SiO_2-D samples were X-ray amorphous. The XRD patterns showed only a very broad peak at $2\Theta \sim 22^\circ$ due to SiO_2. After activation, the XRD patterns depended on the *P*/*V* ratio. Sample VPO/SiO_2-D-1.1 showed a broad peak at $2\Theta = 29.3^\circ$ which could be attributed to either α_I-$VOPO_4$, α_{II}-$VOPO_4$ or $VOPO_4 \cdot xH_2O$. It also showed a weak peak at $2\Theta = 11.5^\circ$ which could be assigned to $VOPO_4 \cdot 2H_2O$. However, patterns collected in an air-tight cell did not show the main peak of α_{II}-$VOPO_4$, $2\Theta = 25^\circ$ [16]. Samples with *P*/*V* ratio greater than 2 were amorphous.

The diffuse reflectance spectra for the VPO/SiO_2-D samples after activation are shown in Figs. 1 and 2. Samples VPO/SiO_2-D-1.1 and VPO/SiO_2-D-2.0 (Fig. 1(a) and (b)) showed an intense asymmetric band that was most likely a combination of two overlapping bands at about 590 and 650 nm. Another major band at about 420 nm was also present, which was absent in the other samples. For sample VPO/SiO_2-D-2.4, two intense bands at greater than 800 nm and 660 nm were observed, together with a weak band at 460 nm (Fig. 1(c)).

The spectra for the ethanol-extracted samples (Fig. 2) were generally similar to that of VPO/SiO_2-D-2.4. The two intense bands in the region above 650 nm were easily observable. The weak band at $\sim$ 460 nm was apparent for sample VPO/SiO_2-D-2.4W, but not for sample VPO/SiO_2-D-2.0W. For

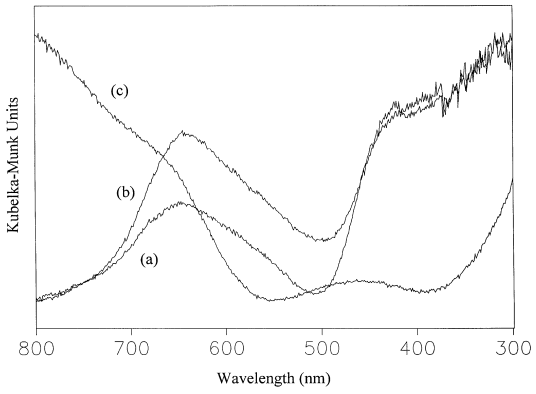

Fig. 1. Diffuse reflectance spectra: (a) VPO/SiO_2-D-1.1, (b) VPO/SiO_2-D-2.0 and (c) VPO/SiO_2-D-2.4.

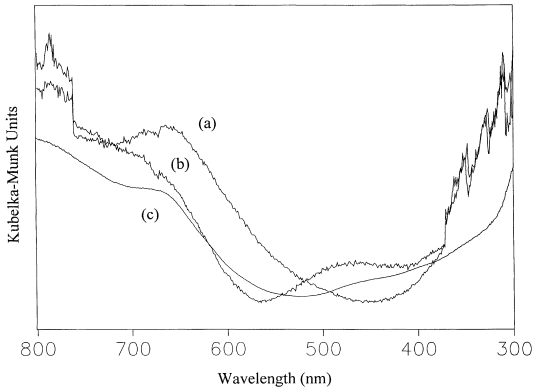

Fig. 2. Diffuse reflectance spectra of ethanol-extracted catalysts: (a) VPO/SiO_2-D-2.0W, (b) VPO/SiO_2-D-2.4W and (c) $VO(PO_3)_2$.

comparison, the spectrum of $VO(PO_3)_2$ is also shown (Fig. 2(c)).

Fig. 3 shows the laser Raman spectra. The spectrum of sample VPO/SiO_2-D-1.1 after activation showed strong bands at 1030 and 942 cm^{-1} and a weak band at 995 cm^{-1}, which indicated the presence of mostly $VOPO_4 \cdot 2H_2O$ (Fig. 3(a)) [16,17]. The LRS spectrum obtained at room temperature after in situ reaction showed strong bands at 1040 cm^{-1} and 920 cm^{-1} with a shoulder at 953 cm^{-1}, which was characteristic of α_I-$VOPO_4$ (Fig. 3(b)) [16]. As shown in Fig. 3(c), a similar spectrum was obtained for the ethanol-washed sample (VPO/SiO_2-D-1.1W). For the ethanol-washed sample VPO/SiO_2-D-2.0W, the LRS spectrum showed a broad peak at 960 cm^{-1} (Fig. 3(d)), which could be

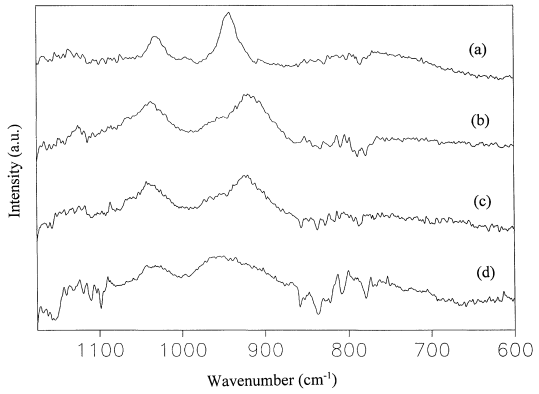

Fig. 3. Room temperature Raman spectra of VPO/SiO_2-D catalysts:(a) VPO/SiO_2-D-1.1 (after activation), (b) VPO/SiO_2-D-1.1 (after in situ reaction),(c) VPO/SiO_2-D-1.1W (after in situ reaction) and(d) VPO/SiO_2-D-2.0W (after in situ reaction).

due to $VO(PO_3)_2$. The latter has main peaks at 961 and 972 cm^{-1} [18].

3.1.2. Reaction data

Table 2 shows the reaction data for the VPO/SiO_2-D samples. Independent of ethanol-washing, the MA selectivity increased with *P/V* ratio until the ratio reached 2.0, thereafter, MA selectivity remained at approximately 50%. Activation temperatures used in this study had a negligible effect on MA selectivity.

3.2. Effect of nature of SiO_2 surface

The effect of the nature of the silica surface was studied with samples prepared on SiO_2–OH and SiO_2–CH_3. Two samples, VPO/SiO_2–OH-1.1 and VPO/SiO_2–CH_3-1.1, were prepared, characterized and compared.

3.2.1. Catalyst characterization

XRD patterns of silica-supported samples and the bulk sample after treatment in air at 500°C for 24 h are shown in Fig. 4(a)–(c). Both silica-supported samples give identical patterns which corresponded to ω-$VOPO_4$ (Fig. 4(a) and (b)) [19], in addition to the broad peak of silica at $2\Theta = 22^\circ$. Patterns collected before and after reaction were identical for both samples with the exception of a weak peak at $2\Theta = 12.5^\circ$ which occasionally appeared. Amoros et al. [20] have reported that ω-$VOPO_4$ rapidly absorbs

Table 2
Reaction data for VPO/SiO_2-D catalysts at 425°C

Activation temperature		475°C				550°C			
Sample[a]	Wt (g)	Conv (%)	Selectivity (%)			Conv (%)	Selectivity (%)		
			MA	CO_2	CO		MA	CO_2	CO
D-1.1	0.18	44	26	19	55	47[b]	23	19	58
D-2.0	0.33	25	50	13	37	37[b]	45	15	38
D-2.4	0.74	11	53	11	36	9[c]	50	38	12
D-1.1W	0.39	32	46	16	38	—	—	—	—
D-2.0W	0.57	28	53	13	34	—	—	—	—
D-2.4W	0.67	20	51	12	37	—	—	—	—
Bulk-1.1	2.0[d]	41	67	11	22	—	—	—	—

[a] Reaction conditions: 41 ml/min, $C_4/O_2/He=2/20/78$.
[b] C_2 and C_3 products were formed.
[c] Catalyst wt.=0.54 g.
[d] Weight of precursor.

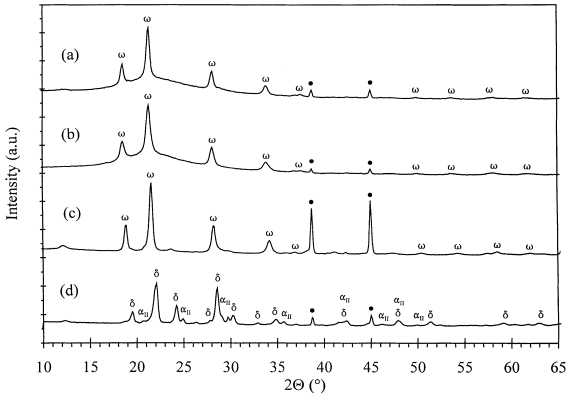

Fig. 4. XRD of samples after air calcination: (a) VPO/SiO_2–CH_3-A, (b) VPO/SiO_2–OH-A, (c) Bulk-A and (d) Bulk-A (after reaction). ω=ω-$VOPO_4$, δ=δ-$VOPO_4$, α_{II}=α_{II}-$VOPO_4$, •=LiF (internal standard).

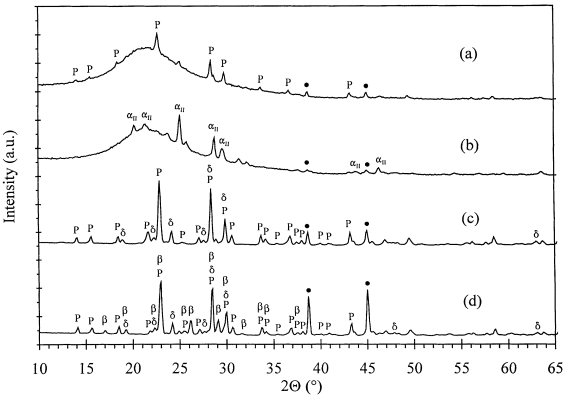

Fig. 5. XRD of samples after air calcination, followed by N_2 calcination for 2 h: (a) VPO/SiO_2–CH_3–N2, (b) VPO/SiO_2–OH–N2, (c) Bulk-N2 and (d) Bulk-N2 (after reaction). P=$(VO)_2P_2O_7$, α_{II}=α_{II}-$VOPO_4$, δ=δ-$VOPO_4$, β=β-$VOPO_4$, •=LiF (internal standard).

water and irreversibly transforms into $VOPO_4{\cdot}2H_2O$. Thus, the 12.5° peak could be a strong diffraction for $VOPO_4{\cdot}2H_2O$. As shown in Fig. 4(c), the bulk sample, Bulk-A, showed similar diffraction peaks to the silica-supported samples, with the exception of seven unidentified, broad, weak peaks at 2Θ =23.6°, 26.3°, 36.0°, 41.1°, 42.3°, 47.4° and 57.5°. The major peaks, however, were slightly shifted towards higher 2Θ values (smaller d-spacing) compared to the silica supported samples. Unlike the supported samples, Bulk-A underwent transformation during reaction (Fig. 4(d)). The dominant species present after reaction was δ-$VOPO_4$ [21] with traces of α_{II}-$VOPO_4$ [16].

Diffraction patterns for samples treated in nitrogen for 2 h at 770°C are shown in Fig. 5. The sample supported on the hydrophobic silica, VPO/SiO_2–CH_3–N2, showed diffraction peaks characteristic of $(VO)_2P_2O_7$ (Fig. 5(a)) at 2Θ=14.1°, 15.5°, 18.4°, 22.7°, 28.4°, 29.8°, 33.7°, 36.7° and 43.2° [16]. There was a small unidentified peak at 58.4°, and the peak at 25.0° appeared to be unusually large to be the (211)

plane of $(VO)_2P_2O_7$ [16]. A small amount of α_{II}-$VOPO_4$, which has a principal diffraction at $2\Theta=25.0^\circ$, may contribute to the latter peak [16]. The sample supported on hydrophilic silica, VPO/SiO_2–OH–N_2, showed peaks attributed to α_{II}-$VOPO_4$ (Fig. 5(b)) in addition to unidentified peaks at $2\Theta=22.7^\circ$, 23.7°, 25.7°, 31.3°, 32.2°, 37.6°, 54.4° and 63.5° [16]. After being used in reaction, two new weak, unidentified peaks appeared ($2\Theta=18.1^\circ$ and 27.4°). The pattern from the bulk sample, Bulk-N_2, corresponded to $(VO)_2P_2O_7$ with a small amount of δ-$VOPO_4$ along with small unidentified peaks at $2\Theta=28.9^\circ$, 46.9°, 49.5°, 58.5° and other weaker peaks at $2\Theta>45.0^\circ$ (Fig. 5(c)) [16,21]. The peak at $2\Theta=28.9^\circ$ might be attributed to one of the main peaks of β-$VOPO_4$, but the other main peak of β-$VOPO_4$ at $2\Theta=26.2^\circ$ was not detected [16]. After being used in reaction, the relative intensities of the peaks changed, the presence of β-$VOPO_4$ became clearly evident, and a small unidentified peak at $2\Theta=24.9^\circ$ appeared [16].

The diffraction patterns for the silica-supported samples treated in nitrogen for 24 h at 770°C are shown in Fig. 6. Both samples showed diffraction peaks, most of which could be attributed to $(VO)_2P_2O_7$ and $VO(SiO)P_2O_7$ [16,22]. By comparing the relative intensities of the strong $VO(SiO)P_2O_7$ peaks ($2\Theta=28.8^\circ$ and 20.3°) to the strong $(VO)_2P_2O_7$ peaks ($2\Theta=28.4^\circ$ and 22.7°), it could be concluded that relatively more $VO(SiO)P_2O_7$ was present in the sample supported on hydrophilic silica (VPO/SiO_2–OH–N24) than in the sample supported on hydrophobic silica (VPO/SiO_2–CH_3–N24).

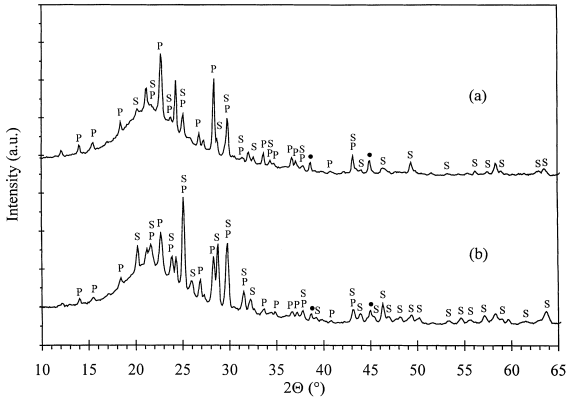

Fig. 6. XRD of samples after air calcination, followed by N_2 calcination for 24 h: (a) VPO/SiO_2–CH_3–N24, (b) VPO/SiO_2–OH–N24. P=$(VO)_2P_2O_7$, S=$(VO)(SiO)P_2O_7$, •=LiF (internal standard).

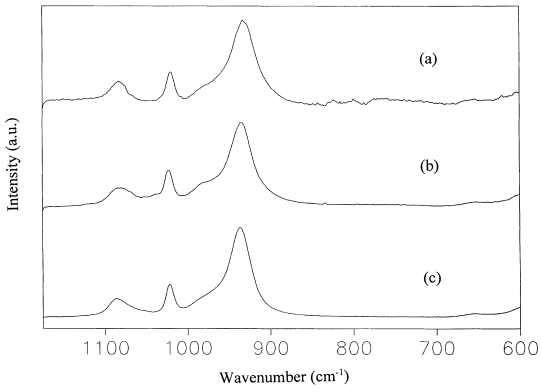

Fig. 7. Room temperature Raman spectra of samples after air calcination:(a) VPO/SiO_2–CH_3-A (after in situ reaction), (b) VPO/SiO_2–OH-A (after in situ reaction) and (c) Bulk-A (after calcination).

Figs. 7 and 8 show the LRS spectra of the silica supported samples calcined in air and treated in nitrogen for 2 h, respectively, at room temperature after in situ reaction at 400°C. The spectra for the bulk catalysts were collected under ambient conditions before reaction. The spectra for the catalysts activated in air are shown in Fig. 7. The spectra for the bulk sample and both silica supported samples showed bands at 934, 979, 1022 and 1083 cm^{-1}. Although

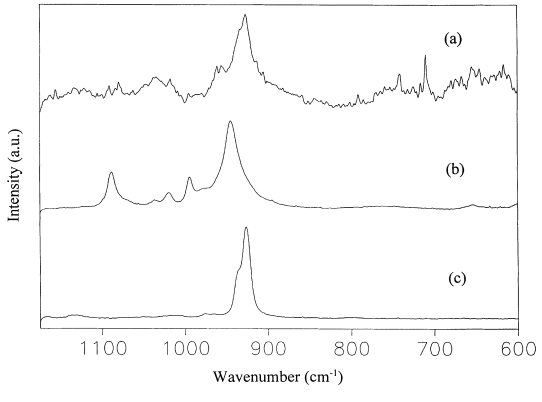

Fig. 8. Room temperature Raman spectra of samples after air calcination, followed by N_2 calcination for 2 h: (a) VPO/SiO_2–CH_3–N2 (after in situ reaction),(b) VPO/SiO_2–OH–N2 (after in situ reaction) and (c) Bulk-N2 (after calcination).

these spectra were similar to those reported for δ-$VOPO_4$ [16], they might be due to ω-$VOPO_4$ for which no spectrum has been reported. The spectrum for the N_2-treated VPO–SiO_2–CH_3–N2 (Fig. 8(a)) showed strong bands at 928 and 933 cm^{-1} which were assigned to the asymmetric P–O–P stretches of $(VO)_2P_2O_7$ [23]. In addition, there might be bands at 950 cm^{-1} and 1025 cm^{-1}, perhaps due to α_I-$VOPO_4$, but the spectrum was too noisy to be definitive [16]. The spectrum for the sample VPO/SiO_2–OH–N2 (Fig. 8(b)) showed bands at 944, 980, 995 and 1089 cm^{-1} which corresponded to α_{II}-$VOPO_4$ [16]. An additional band at 1021 cm^{-1} might be due to δ-$VOPO_4$ [16]. A very weak band at 1036 cm^{-1} remained unidentified. Bulk-N2 showed the characteristic peaks of $(VO)_2P_2O_7$ at 927 and 933 cm^{-1} (Fig. 8(c)) [16].

3.2.2. Reaction data

The reaction data are shown in Table 3. Interestingly, the selectivity for MA on the supported catalysts, 19–27% at 425°C and 17–23% at 485°C, did not differ substantially in spite of the very different crystalline phases detected. The VPO/SiO_2–CH_3 samples were slightly more active than the VPO/SiO_2–OH samples. The activity for sample VPO/SiO_2–CH_3–N24 was much lower than the others, which could be due to loss in surface area and the formation of $VO(SiO)P_2O_7$. In contrast, the Bulk-A sample exhibited 45–55% MA selectivity for butane conversions between 5% and 20% and, Bulk-N2 produced MA with selectivity ranging between 30% and 45% (which varied from batch to batch) at conversions ranging from 5% to 30%.

4. Discussion

4.1. Effect of ethanol extraction and P/V ratio

Catalysts prepared with SiO_2-D show clearly that the nature of the vanadium species depends strongly on the *P*/*V* ratio. The diffuse reflectance spectra of the samples VPO/SiO_2-D-1.1 and VPO/SiO_2-D-2.0 are different from the other samples. The spectra of these other samples are close to that of $VO(PO_3)_2$. They all show strong absorption above 700 nm, which is indicative of the presence of VO^{+2} by comparison with spectra of known compounds (see Table 4). This is consistent with the fact that silica-supported samples of *P*/*V*=2 and higher contain a high concentration of V^{4+} [6] and ethanol preferentially dissolves V^{5+} compounds. By inference, the strong absorption at 590–650 nm of samples VPO/SiO_2-D-1.1 and VPO/SiO_2-D-2.0 is due to V^{5+} oxo species. The presence of $VOPO_4$ is detected by LRS (Fig. 3(a)), and washing the sample with ethanol causes the appearance of a Raman peak at ∼960 cm^{-1} (Fig. 3(c)) which is consistent with preferential removal of $VOPO_4$ by ethanol.

The catalytic data in Table 2 show that ethanol washing increases MA selectivity for sample VPO/SiO_2-D-1.1 substantially, but has much less effect for samples of higher *P*/*V* ratios. This is true in spite of different conversion data being used for comparison, since previous data of such supported VPO catalysts showed that the selectivity only depends weakly on conversion [6,7].

Previously, we have shown that on SiO_2-supported samples, MA selectivity increases with *P*/*V* ratio up to

Table 3
Reaction data for catalysts supported on hydrophilic and hydrophobic silica

Reaction temperature		425°C				485°C			
Sample[a]	Wt (g)	Conv (%)	Selectivity (%)			Conv (%)	Selectivity (%)		
			MA	CO_2	CO		MA	CO_2	CO
VPO/SiO_2–OH–A	0.50	28	27	18	55	72	23	19	58
VPO/SiO_2–OH–N2	0.50	19	19	19	62	53	17	19	64
VPO/SiO_2–CH_3–A	0.46	33	25	19	56	73	21	21	58
VPO/SiO_2–CH_3–N2	0.47	24	24	18	58	60	22	18	60
VPO/SiO_2–CH_3–N24[b]	0.29	10	24	16	60	32	21	19	60

[a] Reaction conditions: 70 ml/min, $C_4/O_2/He$=2/24/74.
[b] 40 ml/min.

Table 4
Absorption bands of some reference compounds[a]

Compound	Medium	Maxima (nm)	Assignment
VO^{+2}	0.5–2 M $HClO_4$	763; 625; 240	$^2B_2 \rightarrow {}^2E(I); {}^2B_2 \rightarrow {}^2B_1; {}^2B_2 \rightarrow {}^2E(II)$
$VOSO_4 \cdot 0.5H_2O$	Crystal(b)	769(⊥); 625; 240(⊥)	$^2B_2 \rightarrow {}^2E(I); {}^2B_2 \rightarrow {}^2B_1; {}^2B_2 \rightarrow {}^2E(II)$
$VOSO_4 \cdot 0.5H_2O$	Powder	775;621	$^2B_2 \rightarrow {}^2E(I); {}^2B_2 \rightarrow {}^2B_1$
VO_2	Powder	240	$^2B_2 \rightarrow {}^2E(II)$
$VO(oxalate)_2^{2-}$	H_2O	794; 606; 340	$^2B_2 \rightarrow {}^2E(I); {}^2B_2 \rightarrow {}^2B_1; {}^2B_2 \rightarrow {}^2A_1$
$VO(tartrate)^{2-}$	H_2O	(909;588); 532; 395	$({}^2B_2 \rightarrow {}^2E(I)); {}^2B_2 \rightarrow {}^2B_1; {}^2B_2 \rightarrow {}^2A_1$

[a] Data extracted from [24].
[b] Light polarized ⊥ to V–O axis.

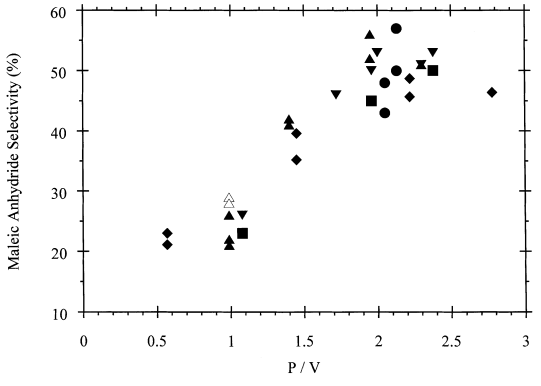

Fig. 9. Effect of *P/V* ratio on MA selectivity over silica-supported VPO prepared and pretreated by various methods, i.e. (starting compounds, silica, pretreatment conditions): ◆=(V/SiO_2 + triethylphosphate, Davisil grade 646, O_2 at T=425°C [7]), ●=($VO(H_2PO_4)_2$, Cab-O-Sil L-90, C_4H_{10}/O_2/He at T=425°C or 485°C [25]), ▼=(V_2O_5 + HCl + H_3PO_4, Davison grade 62, C_4H_{10}/O_2/He at T=475°C [this work]), ■=(V_2O_5 + HCl + H_3PO_4, Davison grade 62, C_4H_{10}/O_2/He at T=550°C [this work]), ▲=(NH_4VO_3 + HO_2CCO_2H + $(NH_4)_2HPO_4$, Davisil grade 644 or 646, air at T=520°C [6]), Δ=(NH_4VO_3 + HO_2CCO_2H + $(NH_4)_2HPO_4$, Davisil grade 644 or 646, C_4H_{10}/O_2/He at T=425°C [6]).

P/V=2.0 [6]. The catalytic data shown in Table 2 are consistent with this trend. In fact, when the collection of catalytic data of SiO_2-supported catalysts are plotted in Fig. 9, the connection between the *P/V* ratio and the MA selectivity is apparent. These data represent samples prepared and pretreated by various methods and for butane conversions from 4% to 44%. Details of the preparation and pretreatment conditions are given in the caption of Fig. 9. Thus, the preparation method, the pretreatment procedures, the nature of the silica or the butane conversion do not have as strong an effect as the *P/V* ratio on the selectivity.

4.2. *Effect of the nature of SiO_2*

The type of silica affects the crystallization process of the VPO compound. When activated in air at 500°C, the SiO_2–OH and SiO_2–CH_3 supported samples and the corresponding unsupported sample form predominantly the same compound, ω-$VOPO_4$. When used in reaction, Bulk-A transforms into δ-$VOPO_4$ and α_{II}-$VOPO_4$, while the supported samples remain unchanged. Further activation in nitrogen at 770°C for 2 h after the air treatment reduces the bulk sample to predominantly $(VO)_2P_2O_7$, agreeing with the results of Hannour et al. [26]. The sample supported on hydrophobic silica, VPO/SiO_2–CH_3–N2, also formed $(VO)_2P_2O_7$, whereas the sample supported on hydrophilic silica, VPO/SiO_2–OH–N2, formed α_{II}-$VOPO_4$ and an unidentified phase(s), but no $(VO)_2P_2O_7$. Formation of $(VO)_2P_2O_7$ requires more extended heating. Thus, the interaction is weaker between VPO and the hydrophobic silica than between the hydrophilic silica. The surface of the hydrophobic silica has been treated with siloxane. It is unlikely that the hydrocarbon chains of the siloxane can survive the calcination at 500°C. Instead, it is more probable that the hydrocarbon chains are oxidized to carbon oxides and water, leaving behind a network of SiO_2 that has few silanol groups. The low density of silanol groups reduces the extent of interaction of VPO with the support surface. The hydrophilic silica surface has a higher density of silanol groups. Thus it interacts more strongly with the VPO compounds.

Extended heating in nitrogen for 24 h causes reaction between SiO_2 and VPO to form $VO(SiO)P_2O_7$. The influence of the stronger support–oxide interaction of the hydrophilic silica is still observable. Sample VPO/SiO_2–OH–N24 shows more $VO(SiO)P_2O_7$ relative to $(VO)_2P_2O_7$ compared with sample VPO/SiO_2–CH_3–N24.

It is quite unexpected that the MA selectivity of sample VPO/SiO_2–CH_3–N2 is only about 25%, even though the sample contains $(VO)_2P_2O_7$ as the predominant crystalline phase. The reason for this is not known. The XRD pattern of the $(VO)_2P_2O_7$ phase agrees quite well with published results [16]. That is, there is no evidence that the morphology of these crystallites are very different from the unsupported $(VO)_2P_2O_7$. It is possible that the surface of the supported $(VO)_2P_2O_7$ is covered with V^{5+} species that are less selective. It is also possible that the supported $(VO)_2P_2O_7$ undergoes oxidation/reduction with different kinetics than unsupported phases, perhaps because of different surface area to volume ratio, or due to interaction with the silica surface. Further investigation is needed to explain this observation.

Finally, it is interesting that calcination of the precursor produces ω-$VOPO_4$. Although this phase is formed for both the unsupported and the supported samples, their XRD peaks are slightly shifted from each other. Hannour et al. [26] have also reported peak shifts for bulk ω-$VOPO_4$ that correspond to variations over ranges of d-spacing for particular diffraction planes . The shifts observed in Bulk-A fall within these ranges [26]. The XRD pattern for the Bulk-A sample corresponds to a contraction along the *a*-axis (from 6.84Å to 6.60Å) and an expansion along the *c*-axis (from 8.42Å to 8.65Å) of ω-$VOPO_4$. Overlap of peaks of ω-$VOPO_4$ and δ-$VOPO_4$ may also contribute to the apparent peak shifts. The 18.4°, 21.2°, 28.1°, 33.8°, 49.8° and 61.6° peaks of ω-$VOPO_4$ [19] are close to the 19.5°, 22.0°, 28.5°, 34.7°, 51.3° and 62.9° peaks of δ-$VOPO_4$ [21].

5. Conclusion

In this study, we have shown that the crystalline phase of VPO formed on a silica support depends upon the type of silica and the extent of interaction of VPO with the silica. Hydrophobic silica interacts less strongly with VPO than hydrophilic silica does, and the transformation of the VPO phase on its surface is more similar to the unsupported VPO. Crystalline $(VO)_2P_2O_7$ can be formed on a hydrophobic silica. However, the MA selectivity of the silica-supported catalysts depends much less on the nature of the silica or the crystalline VPO phases formed than on the *P*/*V* ratio. As was observed previously, selectivity is the highest when the *P*/*V* ratio is about two.

Acknowledgements

This work was supported by the U.S. Department of Energy, Basic Energy Sciences. J.M.C. Bueno acknowledges support from CNPq (Brasil) Conselho Nacional de Desenvolvimento Cientifica e Tecnologico. Cab-O-Sil silica was provided by Cabot Corporation. A. Chu Kung assisted in collecting diffuse reflectance spectra, and G.W. Sutton assisted in collecting reaction data and XRD spectra.

References

[1] G. Centi, F. Trifiro, J.R. Ebner, V.M. Franchetti, Chem. Rev. 88 (1988) 55.
[2] R.A. Overbeek, A.R.C.J. Pekelharing, A.J. van Dillen, J.W. Geus, Appl. Catal. A: general 135 (1996) 231.
[3] R.A. Overbeek, P.A. Warringa, M.J.D. Crombag, L.M. Visser, A.J. van Dillen, J.W. Geus, Appl. Catal. A: general 135 (1996) 209.
[4] V.A. Zazhigalov, Yu.P. Zaitsev, V.M. Belousov, B. Parlitz, W. Hanke, G. Öhlmann, React. Kinet. Catal. Lett. 32 (1986) 209.
[5] M. Martinez-Lara, L. Moreno-Real, R. Pozas-Tormo, A. Jimenez-Lopez, S. Bruque, P. Ruiz, G. Poncelet, Can. J. Chem. 70 (1992) 5.
[6] K.E. Birkeland, S.M. Babitz, G.K. Bethke, H.H. Kung, G.W. Coulston, S.R. Bare, J. Phys. Chem. B 101 (1997) 6895.
[7] W.D. Harding, K.E. Birkeland, H.H. Kung, Catal. Lett. 28 (1994) 1.
[8] W.D. Harding, Ph.D. thesis, Northwestern University, 1993.
[9] K.E. Birkeland, Ph.D. thesis, Northwestern University, 1995.
[10] L. Owens, H.H. Kung, J. Catal. 144 (1993) 202.
[11] Product Literature from Cabot Corporation, Cab-O-Sil Division, Tuscola, IL, USA.
[12] G. Centi, C. Galassi, I. Manenti, A. Riva, F. Trifiro, Preparation of catalysts III: Scientific bases for the preparation of heterogeneous catalysts, in: G. Poncelet, P. Grange, P.A. Jacobs (Eds.), Studies in Surface Science and Catalysis, vol. 16, Elsevier, Amsterdam, 1983, p. 543.

[13] P.J. Andersen, H.H. Kung, J. Phys. Chem. 96 (1992) 3114.
[14] G. Busca, F. Cavani, G. Centi, F. Trifiro, J. Catal. 99 (1986) 400.
[15] G.J. Hutchings, A. Desmartin-Chomel, R. Olier, J.C. Volta, Nature 368 (1994) 41.
[16] F. Ben Abdelouahab, R. Olier, N. Guilhaume, F. Lefebvre, J.C. Volta, J. Catal. 134 (1992) 151.
[17] F. Benabdelouahab, J.C. Volta, R. Olier, J. Catal. 148 (1994) 334.
[18] M.T. Sananes, G.J. Hutchings, J.C. Volta, J. Catal. 154 (1995) 253.
[19] JCPDS file# 37-0809.
[20] P. Amoros, M.D. Marcos, J. Alamo, A. Beltran, D. Beltran, Mat. Res. Soc. Symp. Proc. 346 (1994) 391.
[21] J.W. Johnson, D.C. Johnston, A.J. Jacobson, Proc. 8th Int. Congress on Catalysis, Berlin, preprint B 5.1, 1984.
[22] JCPDS file# 30-1430.
[23] T.P. Moser, G.L. Schrader, J. Catal. 92 (1985) 216.
[24] C.J. Ballhausen, H.B. Gray, Inorg. Chem. 1 (1962) 111.
[25] G.K. Bethke, D. Wang, J.M.C. Bueno, M.C. Kung, H.H. Kung, in: Proc. 3rd World Congress on Oxidation Catalysis, R.K. Grasselli, S.T. Oyama, A.M. Gaffney, J.E. Lyons (Eds.), Studies in surface science and catalysis, vol. 110, Elsevier, Amsterdam, 1997, p. 453.
[26] K. Hannour, A. Lamari, E. Kesteman, N. Duvauchelle, E. Bordes, Abstracts of Posters, 11th International Congress on Catalysis, Baltimore, MD, The North American Catalysis Society, 1996, Poster 246.